Multichannel EEG analysis of respiratory evoked-potential components during wakefulness and NREM sleep

KATE E. WEBSTER AND IAN M. COLRAIN
Department of Psychology, The University of Melbourne, Parkville, Victoria 3052, Australia

Webster, Kate E., and Ian M. Colrain. Multichannel EEG analysis of respiratory evoked-potential components during wakefulness and NREM sleep. *J. Appl. Physiol.* 85(5): 1727–1735, 1998.—Airway occlusion in awake humans produces a somatosensory evoked response called the respiratory-related evoked potential (RREP). In the present study, 29 channel evoked-potential recordings were obtained from seven men who were exposed to 250-ms inspiratory airway occlusions during wakefulness, stage 1, stage 2, and slow-wave sleep. The RREP recorded during wakefulness was similar to previous reports, with the unique observation of an additional short-latency positive peak with a mean latency of 25 ms. Short-latency RREP components were maintained in non-rapid-eye-movement (NREM) sleep. The clearly seen N_1 vertex and late positive complex components during wakefulness were markedly attenuated during NREM sleep, and two large negative components (N_{300} and N_{550}) dominated the sleep RREP. These findings indicate the maintenance of central nervous system monitoring of respiratory afferent information during NREM sleep, presumably to facilitate protective arousal responses to pathophysiological respiratory phenomena.

non-rapid-eye-movement; respiratory-related evoked potential; evoked potentials; somatosensory; respiration; sleep

SLEEP-INDUCED VARIATIONS in human cortical evoked responses have previously been investigated by using auditory, visual, and somatosensory evoked potentials, with the majority of studies using the auditory modality. In general, short-latency auditory components are essentially unchanged between wakefulness and sleep (3); the N_1 vertex component is consistently reported to decrease in amplitude (12, 23); and long-latency components are drastically altered (2). The predominant long-latency components in the sleep-event-related potential consist of a large P_2, occurring at ~200 ms, which is followed by two large negative-going waveforms, the first peaking between 250 and 350 ms (N_{300}) and the second at ~550 ms (N_{550}) (2, 21, 23).

Falling asleep has profound effects on respiratory activity that include reductions in ventilation (4, 5); increases in alveolar P_{CO_2} (29) and upper airway resistance (18); and an impaired ability to compensate for increased resistive loads (15, 17). These observed changes may be due to the absence of the cortical activation of brain stem reticular formation present during wakefulness, known as the wakefulness stimulus (13, 24). The exact nature of this stimulus is unknown; however, it is clear that during wakefulness cortical influences on respiratory neurons are substantial. Furthermore, the loss of this input during sleep may have important consequences, the most extreme being cessation of breathing due to obstruction of the upper airway. The mechanical consequences of airway obstruction produce a number of afferent signals to the cortex from pressure and muscle stretch receptors (10, 11). It is therefore of considerable interest to determine the ability of the nervous system to respond to these signals during sleep.

Brief occlusion of the inspiratory airway in awake humans produces a series of respiratory-related evoked-potential (RREP) components. Initial reports (8, 27) described a response showing four peaks (P_1, N_1, P_2, N_2) recorded from central sites referenced to C_z. There is substantial similarity in the waveform of the RREP to those seen in response to mechanically elicited somatosensory evoked potentials (SEPs) (8). The early components (occurring <100 ms after stimulus presentation) have received primary attention because they are thought to reflect cortical activation of the somatosensory afferent signal (20). The initial positive peak (P_1), which is maximal over postcentral scalp regions (7), has been shown to vary inversely with inspiratory drive (9) and increase with increasing resistive load magnitude (19). A separate, early negative component (N_f) seen over frontal scalp regions has also been reported (7).

Late RREP components can also be produced. Strobel and Daubenspeck (28) report large late components to a negative pressure pulse greater than -5 $cmH_2O \cdot l^{-1} \cdot s$ presented randomly in a series of breaths. When trials were presented on every breath, the late components were either greatly diminished or absent. Harver et al. (16) report data resulting from 200-ms occlusions recorded under "attend" (counting the occluded breaths) and "ignore" (read silently) conditions. A late positive component (P_3) was reliably observed in both conditions but was seen to be larger and earlier in the attend condition.

There has been only one published study to investigate the RREP during sleep. Wheatley and White (30) recorded data from C_z–C_3 and C_z–C_4 montages during wakefulness and stable non-rapid-eye-movement (NREM) sleep (stages 2, 3, and 4 combined). Wakefulness data were consistent with previous studies (8, 27), with four components (P_1, N_1, P_2, and N_2) produced by a negative pressure stimulus at approximate latencies of 72, 128, 231, and 340 ms, respectively (at C_z–C_3). Wheatley and White reported a very different waveform during sleep, in which they were able to identify three peaks that they labeled P_1, N_1, and P_2. The sleep P_1 was seen at ~116 ms. The sleep N_1 was a broad negative deflection lasting ~400 ms, with a peak value of ~10 μV at 244 ms. The sleep P_2 at 664 ms immediately followed the N_1 and was also large (14 μV).

The above-mentioned authors suggest that the P_1 observed during wakefulness is preserved in sleep but is substantially delayed, whereas N_1, P_2, and N_2 no

longer occur during sleep and are replaced by the sleep-specific K-complex response. An alternative explanation is that the P_1 observed during sleep is the P_{200} component typically seen at the start of the sleep N_{300} component and is unrelated to the P_1 seen during wakefulness. This would mean that the early components of the RREP either are not produced during sleep or were obscured by the high-amplitude background activity associated with slow-wave sleep (SWS).

The present study was designed to further evaluate the effect of NREM sleep on RREP components produced in response to brief inspiratory occlusion, using multiple electroencephalographic (EEG) channels and separately investigating each NREM sleep stage. On the basis of the findings of Wheatley and White (30), it was hypothesized that RREP components would be markedly altered from wakefulness to sleep. Specifically, component latencies will be prolonged and amplitudes increased.

METHODS

Subjects. Recordings were obtained from seven men (age range 19–28 yr). All were nonsmokers and reported no history of respiratory or sleep disorders. The laboratory procedures were approved by the University of Melbourne's Human Subjects Ethics Committee.

Respiratory stimuli. Respiratory equipment consisted of a face mask (Hans Rudolf series 7940) connected to a nonrebreathing valve (Hans Rudolf series 2600), supported by a suspending cable. Inspiratory airflow was measured by using a Fleisch pneumotachograph, a Validyne DP 45–14 pressure transducer, and a Validyne CD15 carrier demodulator. The signal was digitized and continuously displayed on a computer monitor by using Compumedics hardware and software. Mask pressure (Pmask) was sampled at a port on the collar connecting the mask to the nonrebreathing valve and was measured by using a second Validyne pressure transducer. Inspiration was interrupted by manual activation of the occlusion valve (Hans Rudolf 2100) at the end of the inspiratory line. Occlusions set to last for 250 ms were presented every three to five breaths.

Digital recording. EEG activity was recorded from 29 scalp sites (FP_1, FP_2, F_7, F_3, F_z, F_4, F_8, FT_7, FT_8, FC_3, FC_z, FC_4, T_3, C_3, C_z, C_4, T_4, TP_7, CP_3, CP_z, CP_4, TP_8, T_5, P_3, P_z, P_4, T_6, O_1, and O_2) on the basis of the International 10/20 system, with all leads referenced to linked ears. Vertical and horizontal electrooculograms (EOG) and a submentalis electromyogram (EMG) were also recorded. The Neuroscan system recorded all EEG sites, both EOG channels, and Pmask with a sampling rate of 1,000 Hz as 1-s evoked-potential epochs with a 100-ms prestimulus baseline. The Pmask signal was attenuated 20,000 times before input to the Neuroscan amplifier. EEG and Pmask were recorded with band-pass filters set to 0.1–100 Hz and a range of ±2.25 μV. The Compumedics system continuously recorded C_3, O_2, EOG, and EMG signals with a sampling rate of 500 Hz. EEG was band passed between 0.1 and 40 Hz with a range of ±125 μV, EOG between 0.1 and 40 Hz with a range of ±250 μV, and EMG between 3 and 40 Hz with a range of ±125 μV. All recorded data were 50-Hz notch filtered. Resistance was below 5 kΩ for all electrode sites.

Procedure. Each subject spent two nights in the laboratory, the first being an adaptation night. On the experimental night, 4 series of 200 occlusion trials were conducted. *Series 1* was conducted while the subject was awake. Three series were carried out during sleep: *series 2* during stage 1 sleep (or sleep onset), *series 3* during stage 2 sleep, and *series 4* during SWS (stages 3 and 4 combined).

Data analysis. Sleep stage was determined by an experienced sleep researcher according to the guidelines of Rechtschaffen and Kales (26). Stages 3 and 4 were combined as SWS. RREPs were averaged separately for each arousal state (i.e., wakefulness, stage 1, stage 2, and SWS), within each subject. An individual trial was included in the average if the occlusion produced a substantial change in Pmask. All epochs not contaminated by eye movement were included for averaging.

Data from all 29 scalp sites were used for topographic mapping. For component analysis, the amplitude and latency of the peaks of the RREP were determined from a reduced set of 15 scalp sites (F_3, F_z, F_4, FC_3, FC_z, FC_4, C_3, C_z, C_4, CP_3, CP_z, CP_4, P_3, P_z, and P_4). Because of the absence of lateralization effects, adjacent sites were grouped together to form five anterior-posterior (A-P) regions for statistical analysis. These consisted of frontal (F_3, F_z, and F_4), frontocentral (FC_3, FC_z, and FC_4), central (C_3, C_z, and C_4), centroparietal (CP_3, CP_z, and CP_4), and parietal (P_3, P_z, and P_4) regions.

P_1 and N_f were defined as the maximal positive and negative deflections, respectively, occurring between 40 and 60 ms after stimulus onset. An additional early positive peak was observed immediately before N_f. This was labeled P_{1a}. N_1 was selected on the basis of being the next negative deflection after these early components at ~100 ms. P_2 and the late positive complex (LPC) were then identified as the following positive deflections. During sleep, N_{300} was identified as the negative peak after P_2, LPC as the positivity after N_{300}, and N_{550} as the next, large negative deflection. All latencies were expressed relative to the start of Pmask change, which occurred 40 ms after valve closure. This was due to the elasticity of the air inside the 3 m of tubing between the occlusion valve and the face mask.

Statistical analysis. The data were analyzed by using a two-factor, repeated-measures analysis of variance to assess the effects of arousal state and A-P region.

RESULTS

Pmask signals for wakefulness, stage 1, stage 2, and SWS are displayed in Fig. 1.

Evoked potentials during wakefulness. Figure 2 displays the RREP waveform recorded during wakefulness. It shows grand averages for all subjects at F_3, F_4, FC_3, FC_4, C_3, C_4, CP_3, CP_4, P_3, and P_4 electrode sites. The RREP waveform varied according to electrode position, with marked differences in the waveform between precentral and postcentral electrode locations, which are detailed below. A series of three early-latency RREP components was observed. A positivity at ~25 ms (P_{1a}), a negativity at ~43 ms (N_f), and a positivity at ~58 ms (P_1). These peaks were present in all subjects, and the mean amplitudes and latencies are summarized in Tables 1 and 2, respectively.

The largest amplitudes for both positive components were recorded from centroparietal electrode sites (CP_3, CP_z, CP_4); however, the main effect of the A-P region was nonsignificant [P_{1a}: $F(4,24) = 3.09$, $P = 0.09$; P_1: $F(4,24) = 3.9$, $P = 0.08$]. The negative component, which separated the two positive components (N_f), showed a strong regional effect, in which frontal locations exhibited the greatest amplitudes [$F(4,24) = 42.2$,

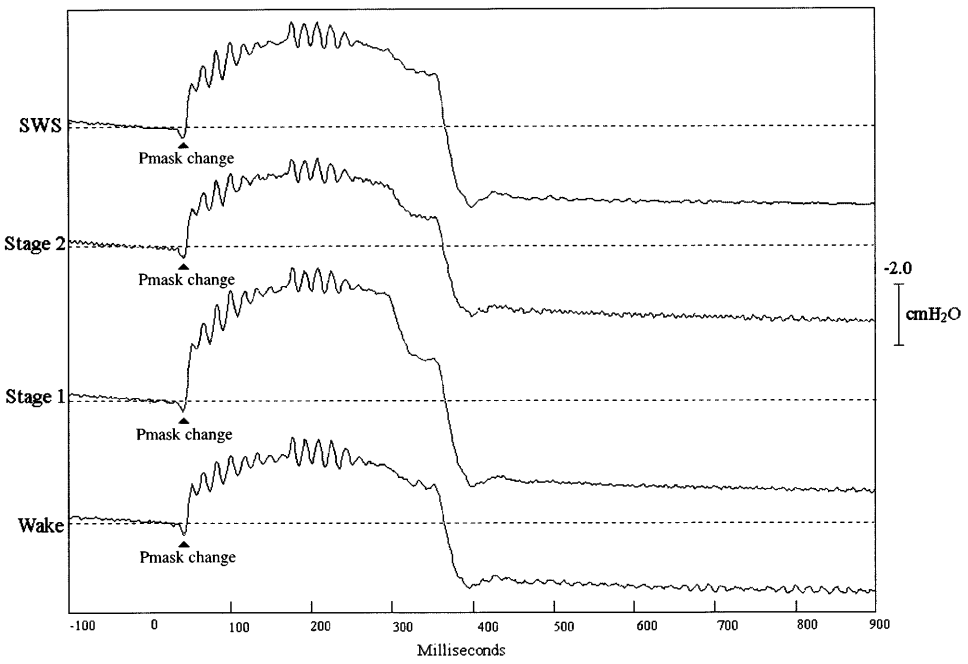

Fig. 1. Grand mean mask pressure (Pmask) signals recorded in response to occlusions in wakefulness, stage 1, stage 2, and slow-wave sleep (SWS). The point of rapid change in Pmask indicates occlusion onset and was used as *time 0* for determining peak latencies.

$P < 0.0001$]. P_{1a} latency displayed a nonsignificant frontal-to-parietal increase [$F(4,24) = 4.25$, $P > 0.05$], whereas P_1 and N_f latencies did not vary with scalp region (Table 2). Topographic maps (Fig. 3*A*) of the two positive components indicated a broad caudal focus, whereas the map of the N_f peak showed a predominant frontal focus, similar to that previously reported by Davenport et al. (7) in children.

N_1, P_2, and LPC components were also identified during wakefulness. Mean amplitudes and latencies

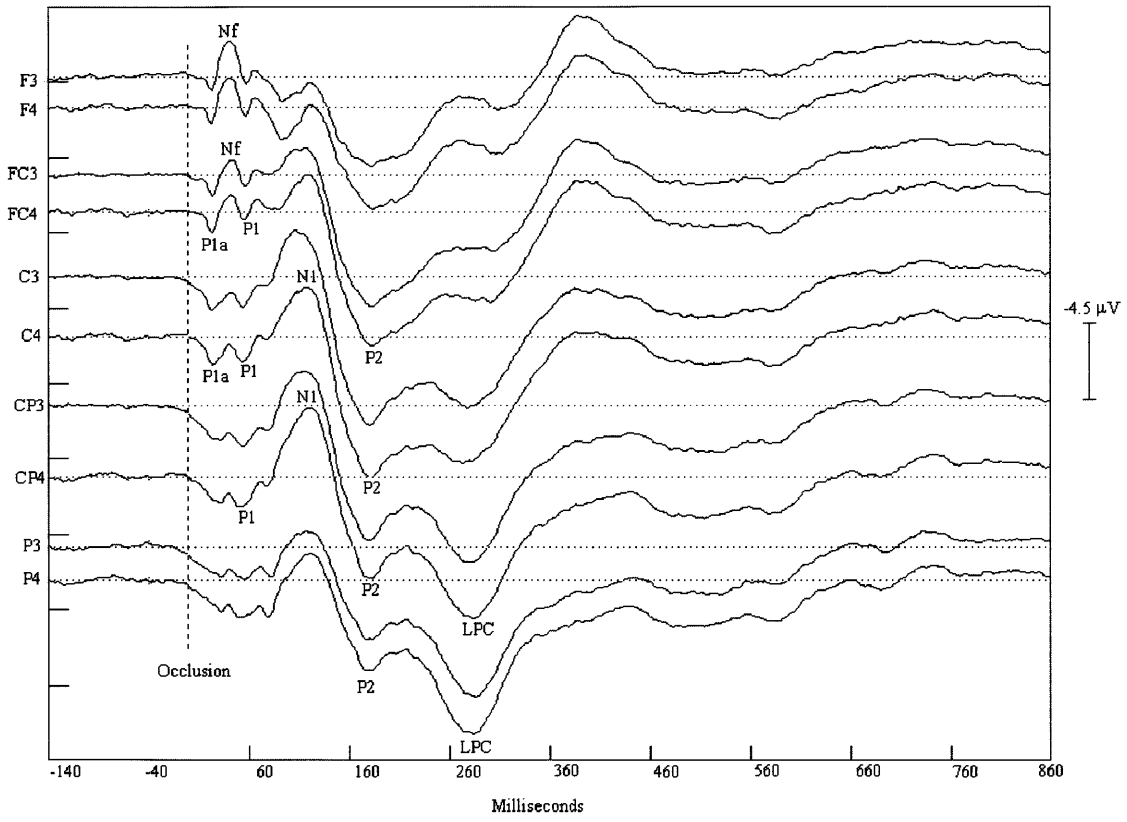

Fig. 2. Grand mean evoked potentials during wakefulness recorded at F_3, F_4, FC_3, FC_4, C_3, C_4, CP_3, CP_4, P_3, and P_4. P_{1a}, N_f, P_1, N_1, P_2, and late positive complex (LPC) peaks are shown, and data are plotted for 140 ms before and 860 ms after Pmask change. Positive voltage is plotted down *y*-axis. See METHODS for details.

Table 1. *RREP peak amplitudes*

	Wakefulness					Stage 1					Stage 2				
	Frontal	Frontocentral	Central	Centroparietal	Parietal	Frontal	Frontocentral	Central	Centroparietal	Parietal	Frontal	Frontocentral	Central	Centroparietal	Parietal
P_{1a}	1.43	1.85	2.56	2.66	2.22	2.45	2.84	2.93	3.26	2.81	1.63	2.20	2.63	3.01	2.45
	±1.38	±1.22	±1.29	±1.06	±1.46	±1.29	±1.04	±0.88	±1.22	±1.49	±2.37	±1.80	±2.40	±2.08	±2.20
N_f	−2.23	−1.48	−0.20	0.31	−0.01	−1.87	−1.19	−0.05	0.91	0.87	0.17	0.75	1.96	2.80	2.10
	±1.46	±1.67	±1.58	±1.45	±1.86	±1.32	±1.61	±1.40	±1.39	±1.80	±2.40	±2.39	±2.49	±2.92	±2.78
P_1	0.92	1.57	3.05	3.74	3.39	1.48	2.22	2.92	3.65	2.97	1.97	2.51	3.33	3.73	3.51
	±3.30	±3.66	±4.26	±3.97	±3.46	±1.47	±2.16	±2.83	±2.64	±2.66	±1.91	±1.28	±1.30	±1.62	±2.06
N_1	−3.00	−4.40	−4.51	−3.66	−2.25	−1.90	−2.02	−2.90	−2.12	−1.79	1.87	1.05	1.04	1.29	0.71
	±3.06	±4.12	±4.16	±3.72	±3.34	±2.64	±2.15	±2.08	±1.91	±1.31	±1.95	±2.11	±1.66	±2.30	±2.25
P_2	6.45	9.35	10.79	9.11	6.95	7.06	8.38	7.11	6.21	5.38	6.48	6.93	7.08	6.25	4.48
	±2.70	±5.09	±5.64	±4.97	±3.07	±1.16	±1.48	±1.91	±2.34	±1.97	±2.83	±3.52	±3.07	±4.47	±3.91
LPC	4.61	7.27	9.63	10.74	11.11	2.85	4.03	5.21	8.43	9.53	−2.73	−3.40	−3.24	−2.67	−1.38
	±3.11	±3.83	±2.55	±1.84	±1.89	±4.99	±7.12	±7.16	±8.77	±7.87	±5.08	±6.58	±5.99	±6.41	±5.58

Values are means ± SD expressed in μV. RREP, respiratory-related evoked potential. P_{1a}, P_1, and P_2: short-latency positive peak with a mean latency of 25 ms, 1st positive peak, and 2nd positive peak, respectively; N_f and N_1, frontally maximal negative peak and 1st negative peak, respectively; LPC, late positive complex.

Table 2. *RREP peak latencies*

	Wakefulness					Stage 1					Stage 2				
	Frontal	Frontocentral	Central	Centroparietal	Parietal	Frontal	Frontocentral	Central	Centroparietal	Parietal	Frontal	Frontocentral	Central	Centroparietal	Parietal
P_{1a}	23.64	23.89	25.17	25.77	27.07	25.05	26.31	27.40	29.68	31.81	29.38	31.46	32.59	33.91	34.07
	±1.22	±1.99	±3.89	±4.33	±4.03	±1.36	±2.97	±4.03	±3.79	±4.49	±5.36	±5.35	±4.85	±6.18	±5.69
N_f	42.54	42.79	42.38	42.53	43.00	43.51	44.33	44.57	44.89	44.43	44.46	45.05	46.10	47.06	48.70
	±4.26	±3.87	±3.06	±2.72	±3.74	±2.06	±2.52	±2.34	±2.38	±2.75	±2.92	±3.05	±2.88	±3.29	±4.35
P_1	58.24	57.72	57.45	57.69	57.69	58.03	58.02	57.14	57.83	58.84	61.12	60.54	59.73	59.38	63.24
	±4.36	±4.66	±5.93	±6.79	±7.17	±2.33	±2.51	±2.80	±3.90	±6.63	±5.50	±4.14	±1.90	±2.03	±7.76
N_1	110.98	112.53	109.65	113.03	111.15	105.75	107.30	108.31	108.88	110.06	105.01	104.61	104.48	105.41	107.25
	±7.54	±7.35	±8.12	±9.00	±11.73	±8.63	±7.16	±7.44	±10.17	±14.31	±7.34	±7.92	±6.14	±6.07	±5.86
P_2	170.95	174.67	175.95	176.71	178.97	167.63	167.47	166.28	169.76	171.10	173.73	172.66	172.98	173.60	173.58
	±8.83	±9.35	±10.24	±9.86	±10.67	±10.44	±10.82	±16.45	±11.69	±11.72	±15.56	±12.61	±11.28	±10.10	±9.84
LPC	292.96	296.11	285.55	283.86	288.72	294.17	298.70	293.90	296.46	291.82	347.70	354.72	357.40	360.46	356.22
	±18.3	±14.96	±15.88	±12.21	±13.30	±18.8	±20.8	±22.5	±15.75	±14.98	±12.36	±19.80	±19.60	±18.50	±17.78

Values are means ± SD expressed in ms.

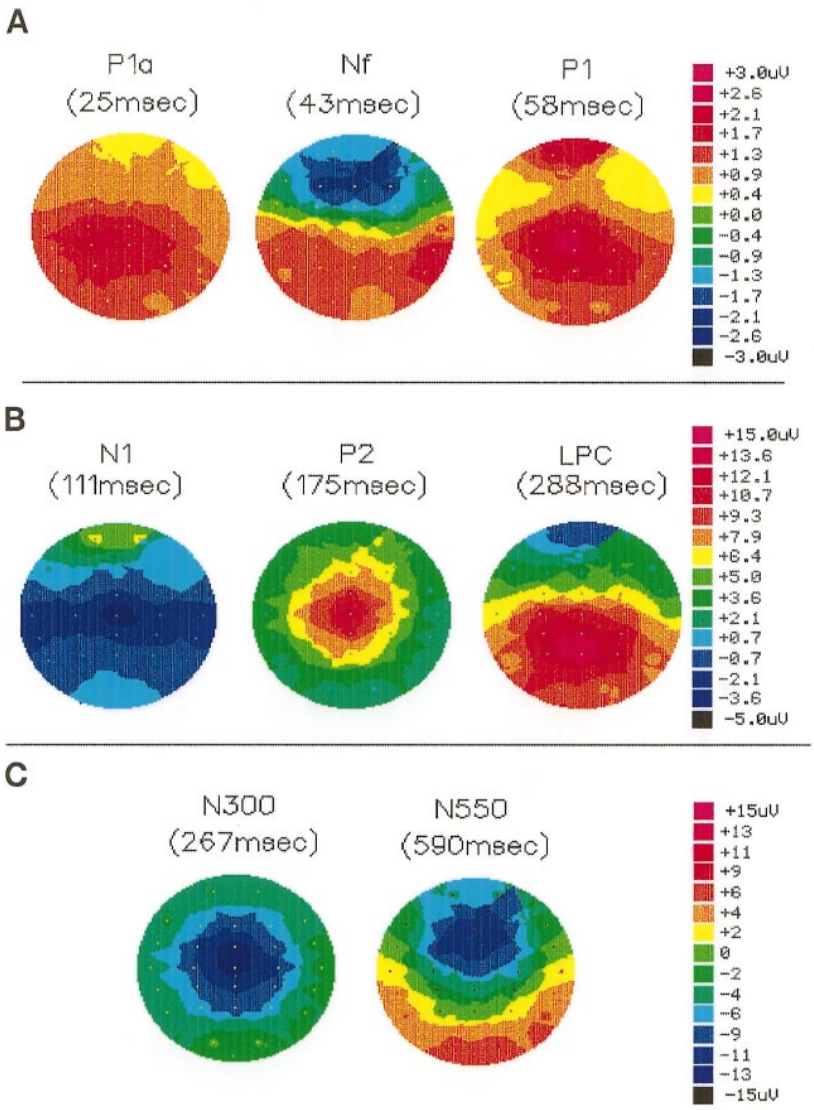

Fig. 3. Topographic representations of EEG voltages at latencies corresponding to peaks of different respiratory-related evoked potential (RREP) components. Voltage values are taken from grand mean evoked potentials. Maps represent a top-down view of head; *top* of each map represents front of head. *A*: P_{1a}, N_f, and P_1 peaks during wakefulness. *B*: N_1, P_2, and LPC peaks during wakefulness. *C*: negative components peaking between 250 and 350 ms (N_{300}) and at ~550 ms (N_{550}) peaks during stage 2 sleep. Note that voltage scales are different in each panel.

are summarized in Tables 1 and 2. The N_1 peak was seen at ~111 ms and was found in all subjects (Fig. 2). The topographic map of N_1 displays a negative band overlying the scalp midline in the general area of the sensorimotor strip (C_3, C_z, and C_4) (Fig. 3*B*). P_2 was centrally maximal [$F(4,24) = 7.46$, $P < 0.01$], with a mean peak latency of 175 ms. The LPC occurred at ~288 ms. This component showed a maximal parietal focus [$F(4,24) = 61.24$, $P < 0.0001$], and a topographic distribution indicative of it being a P_{300} response (Fig. 3*B*).

Evoked potentials during NREM sleep. P_{1a}, N_f, and P_1 components were not identifiable in SWS, and thus statistical analysis was limited to wakefulness, stage 1, and stage 2 sleep. The waveforms for the early-latency components at F_z and C_z, across arousal states, is displayed in Fig. 4.

From the mean latency values in Table 2, it is clear that both P_{1a} and N_f latencies increased significantly from wakefulness to sleep stages 1 and 2 [$F(2,12) = 35.4$, $P < 0.0001$ and $F(2,12) = 6.6$, $P < 0.05$, respectively]. P_1 latency was unchanged between wakefulness and stage 1 sleep. Planned contrasts, however, showed a significant latency increase from stage 1 to stage 2 sleep [$t(1) = 6.07$, $P < 0.05$]. P_{1a} and P_1 amplitudes were unaffected by arousal state [$F(2,12) = 0.344$, $P > 0.05$; $F(2,12) = 1.79$, $P > 0.05$, respectively]. N_f showed a nonsignificant trend of decreasing amplitudes with the progression of sleep [$F(2,12) = 0.736$, $P > 0.05$]. However, the general positive drift of the waveform during stage 2 sleep should be noted (Fig. 4).

Figure 5 displays long-latency RREP components at C_z and P_z during wakefulness, stage 1, stage 2, and SWS. The N_1 component showed a significant decrease in amplitude with sleep and was nonexistent in three subjects during SWS [$F(2,12) = 5.89$, $P < 0.05$]. There was no significant difference in arousal state for N_1 latency [$F(2,12) = 1.98$, $P > 0.05$]. The P_2 component remained present during sleep with no significant reduction in amplitude or latency [$F(2,12) = 0.96$, $P >$

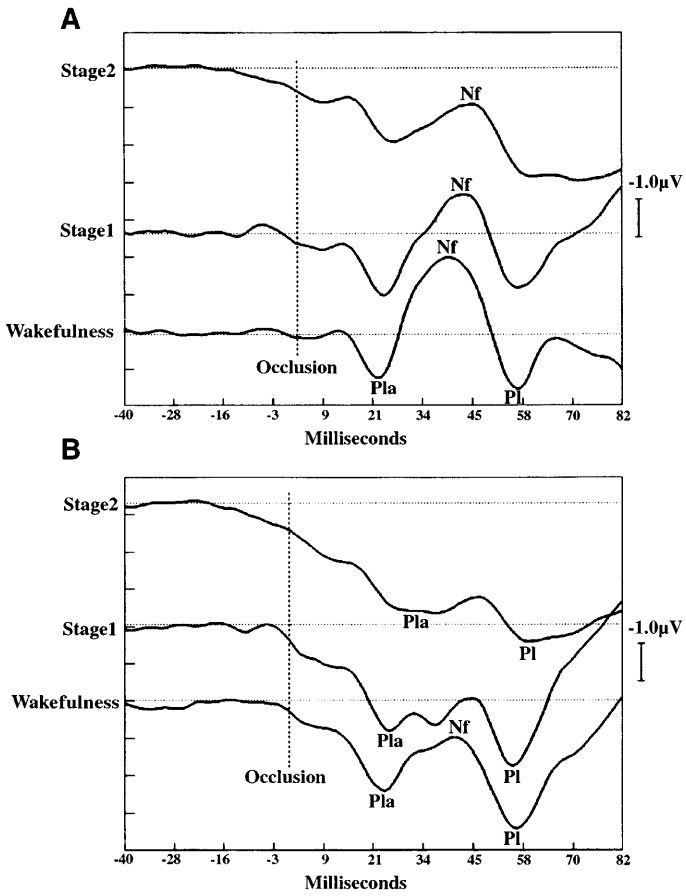

Fig. 4. Grand mean evoked potentials during wakefulness, stage 1, and stage 2 sleep recorded at F_z (*A*) and C_z (*B*). P_{1a}, N_f, and P_1 peaks are shown, and data are plotted for 40 ms before and 82 ms after Pmask change. Positive voltage is plotted down *y*-axis.

0.05 and $F(2,12) = 0.757$, $P > 0.05$, respectively]. However, there was a trend toward decreasing amplitudes with the progression of sleep, and this was best seen at the central electrode sites where the component was maximal. The prominent LPC (best seen parietally) observed during wakefulness was markedly reduced during stage 1 and stage 2 sleep [$F(2,12) = 8.323$, $P < 0.05$] and was not reliably detected during SWS. LPC latency also underwent marked changes, with the component occurring at ~288 ms during wakefulness and increasing to ~355 ms in stage 2 sleep [$F(2,12) = 28.85$, $P < 0.001$] (Table 2).

During stage 2 and SWS, clearly the most predominant components of the RREP waveform were a central dominant N_{300} and a frontocentral dominant N_{550} (Figs. 3*C* and 5). Amplitude and latency values for both components during stage 2 and SWS are displayed in Table 3. The main effect of the A-P region for N_{300} amplitude was nonsignificant [$F(4,24) = 0.95$, $P > 0.05$]; however, the largest values were recorded from central electrode sites (see Table 3). N_{550} amplitude showed a significant main effect of the A-P region [$F(4,24) = 28.75$, $P < 0.0001$], with maximal values at the frontocentral electrode sites.

From Table 3 it can also be seen that both components showed clear intersubject variability in terms of latency, especially during SWS. Despite such variability, N_{300} latency values significantly increased from stage 2 to SWS [$F(1,6) = 20.34$, $P < 0.001$], whereas N_{550} occurred earlier in SWS than in stage 2 [$F(1,6) = 7.61$, $P > 0.05$].

DISCUSSION

The results of the present study demonstrate that, during wakefulness, brief occlusion of the inspiratory airway produces a series of three early-latency peaks (P_{1a}, N_f, and P_1), together with three later-occurring peaks (N_1, P_2, and LPC). During stage 2 sleep, the early response appears to be maintained; however, the later-occurring N_1 and LPC components are markedly reduced, and the response is dominated by two large, negative components (N_{300} and N_{550}).

Early components. The first identified positive component, labeled P_{1a} in the present study, had a mean peak latency of 25 ms at central scalp sites. There was, however, variation among subjects, with latency values ranging from 19 to 31 ms. Such latencies make the interpretation of P_{1a} difficult. Components that occur at 30 ms may well be cortically generated; however, components at 19 ms may also be interpreted as more likely having been produced subcortically.

This is the first study to have identified three early-latency components, with the majority of previous studies having identified only the P_1 component. Such a

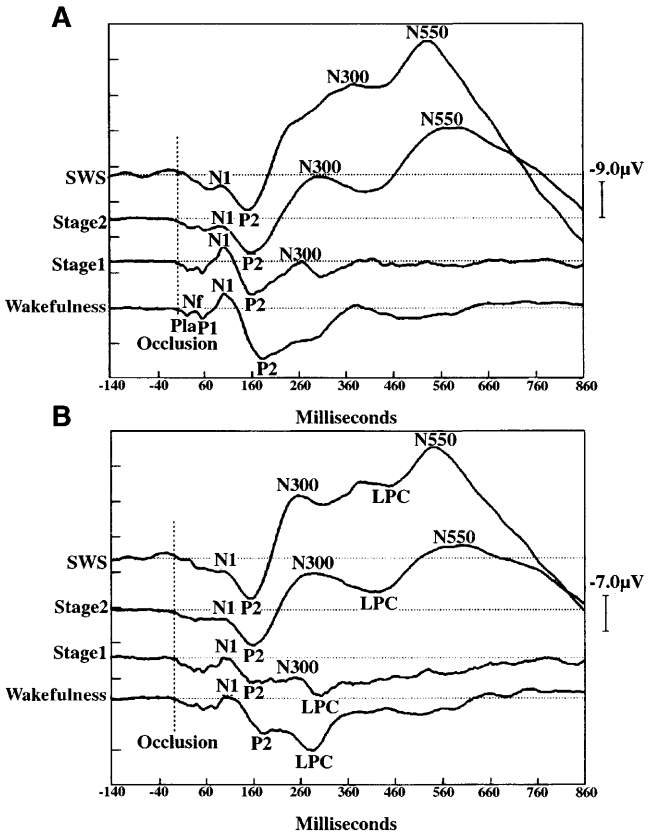

Fig. 5. Grand mean evoked potentials during wakefulness, stage 1, stage 2, and SWS recorded at C_z (*A*) and P_z (*B*). P_{1a}, N_f, P_1, N_1, P_2, LPC, N_{300}, and N_{550} peaks are shown, and data are plotted for 140 ms before and 860 ms after Pmask change. Positive voltage is plotted down *y*-axis.

Table 3. *RREP amplitude and latency values for N_{300} and N_{550} during stage 2 and slow-wave sleep*

	Stage 2					SWS				
	Frontal	Frontocentral	Central	Centroparietal	Parietal	Frontal	Frontocentral	Central	Centroparietal	Parietal
Amplitude, μV										
N_{300}	−4.90	−8.33	−8.83	−8.22	−5.24	−11.40	−12.35	−15.32	−10.01	−8.80
	±4.7	±5.23	±5.69	±4.95	±4.71	±5.09	±6.28	±5.07	±4.45	±4.78
N_{550}	−27.47	−31.46	−25.19	−19.11	−14.45	−25.47	−28.05	−24.82	−19.56	−15.32
	±15.21	±17.93	±16.74	±19.20	±12.74	±5.09	±6.28	±12.95	±12.18	±10.53
Latency, ms										
N_{300}	264.31	264.19	275.02	266.73	267.03	319.68	327.01	336.30	324.89	320.49
	±24.98	±16.38	±17.78	±19.49	±14.84	±47.75	±34.79	±28.66	±32.77	±37.80
N_{550}	591.68	590.12	590.02	586.14	586.03	555.03	554.88	554.95	555.89	558.31
	±14.20	±13.60	±13.68	±15.87	±16.71	±28.22	±28.51	±28.25	±26.12	±24.45

Values are means ± SD. N_{300} and N_{550}, negative waveforms peaking between 250 and 350 ms and at ~550 ms, respectively; SWS, slow-wave sleep.

difference may be due to the use of a face mask in the present study, whereas previous studies have used a mouthpiece and nose clip. The use of a face mask allows the possibility of increased trigeminal afferent stimulation and stimulation of negative pressure receptors in the nasal cavity. The role of trigeminal and upper airway receptors in the generation of early RREP components, however, is yet to be fully determined.

P_1 (reported presently) has a latency consistent with studies previously reported using similar elicitation procedures in adult subjects (19, 27). This would appear to confirm the suggestion made by Davenport et al. (7) that their shorter-latency P_1 (29 ms) was due to using children as subjects and not to the use of a linked-ear reference. Davenport et al. (7) reported P_1 as having a parietally maximal topography and identified a frontally maximal negative component that they labeled as N_f. The authors hypothesized that the frontal distribution of the peak suggested a second cortical generator, possibly in the motor cortex. The present investigation confirmed the presence of a frontally maximal N_f component during wakefulness and stage 1 and stage 2 sleep.

This finding has interesting implications concerning the generators of these early components. The activation of multiple early SEP generators has gained considerable support from recent studies. Peterson et al. (25) performed detailed epidural and intracortical mapping of somatosensory evoked activity in Old World monkeys. They reported that their data indicated parallel-component generation by pre- and postcentral dipoles for early-latency mechanical and electrical SEPs. Clearly, the present data are most in agreement with the results of Peterson et al. and thus the multiple-generator hypothesis. A recent study utilizing source-localization analysis has attempted to further investigate the origin of these early peaks (20). The same three early-latency peaks (P_{1a}, N_f, and P_1) were identified at similar latencies. Source-localization analysis failed to model the earliest positive component as a cortically generated component. N_f was localized to the supplementary motor cortex and P_1 to the primary somatosensory cortex.

The data indicate that the early RREP components identified during wakefulness are maintained into stage 2 sleep, with no significant changes in amplitude. Although this result is superficially at odds with the Wheatley and White (30) finding, it can be considered as not inconsistent with their result given the major methodological differences between the two studies. The present data display no clear early components during SWS. Given that Wheatley and White report that their NREM data were averaged from stages 2, 3, and 4 sleep, it is not unsurprising that short-latency components were not apparent in their sleep data. Second, they used bipolar montages comparing C_3 and C_4 to the C_z electrode. The topographic data from the present study show the similarity between C_z and the other central sites. Thus it is possible that, during sleep, with the consequently higher background noise levels in the EEG, the bipolar montages were not sufficiently sensitive to show the early components.

It is meaningful to note that results concerning the effect of NREM sleep on short-latency (nonrespiratory) somatosensory evoked potentials have been equivocal. Although some have emphasized the stability of the short-latency components between wakefulness and sleep (22), others report prolonged latencies, reduced amplitudes, and altered waveforms (e.g., Refs. 1 and 14). However, the magnitude of the latency change is typically on the order of 4 ms (1) and thus much less than the 38 ms reported by Wheatley and White (30) for P_1.

In light of the present data and the literature on SEP, it would appear sensible to reinterpret the Wheatley and White (30) result. First, they failed to see any early components during NREM sleep because of the inclusion of SWS and the use of bipolar recordings. Second, their reporting of a late P_1 is, in fact, a mislabeling of the P_2 preceding the sleep-specific N_{300} (clearly observable in their data).

Late components. The N_1 component occurs ~100 ms after stimulus presentation and as such falls on the border between the early and late responses. The topographic map of N_1 during wakefulness is worthy of comment. A broad negative band was observed to overlie the scalp midline in the general area of the central sulcus. This would suggest the component results from broad activation of the somatosensory cortex and strongly supports the argument that the

occlusion stimulus results in a somatosensory evoked potential. Conclusions of different studies that have measured N_1 to auditory stimuli during sleep are in fairly good agreement. Typically, the amplitude of N_1 decreases in sleep, being almost nonexistent during SWS, whereas N_1 latency shows no apparent change (12, 23). This was also the case for the present findings, in which N_1 was seen to significantly decrease during SWS and was nonexistent in three of the seven subjects.

The late negativity apparent in the wakefulness waveform at ~400 ms is difficult to interpret. It may reflect a response to the offset of the stimulus. Further evaluation of this hypothesis will require the use of stimuli of different durations.

Two large negative components, N_{300} and N_{550}, which are not present during wakefulness, are prominent in NREM sleep. The LPC, N_{300}, and N_{550} data are consistent with those for auditory evoked potentials (6). As with the present data, the auditory N_{300} typically displays increases in amplitude and latency in stage 1 sleep and then more marked increases in stage 2 sleep (21, 23). The interpretation of the N_{300} and N_{550} components has been debated in the context of the auditory literature. Specifically, two contrary views have been developed as to whether these components and the K complexes they relate to reflect an arousal or sleep-maintenance process. What is clear, however, is that they reflect some form of cortical processing of stimuli that is specific to NREM sleep.

The N_{550} component in the present data is not seen until stage 2 sleep. This is also the case with auditory evoked responses (2). The topography of the N_{300} and N_{550} components has been shown to be identical in both respiratory and auditory evoked potentials during stage 2 sleep (6), and thus these components would seem to reflect sleep-specific, modality-independent processes.

Early-latency RREP components appear to be similar during light sleep and wakefulness. This would indicate that afferent transmission to somatosensory and motor cortexes is maintained during NREM sleep, presumably to allow for further processing of stimuli associated with increased airway resistance. N_1 is greatly diminished, starting in stage 1. The LPC, which probably reflects a P_{300} during wakefulness, undergoes a substantial increase in latency with sleep onset and is almost certainly a different component during NREM sleep. During wakefulness, N_1 and P_{300} are considered to reflect endogenous or cognitive processing of stimuli and are influenced by variables that impact on attention and memory. It is thus not surprising that during sleep they are greatly altered. From the waveforms in Fig. 5, stage 1 sleep appears to be an intermediate stage between wakefulness and stage 2. This is likely to reflect the typical oscillation between alpha and theta EEG frequencies characteristic of the sleep-onset period (4, 5, 15, 18, 29). However, a more systematic investigation of this stage is warranted.

The present investigation provides evidence that the cortical response to short-latency RREP components is protected in sleep. These data suggest maintenance of afferent sensory processing of respiratory stimuli during sleep, similar in nature to that seen in the sensory components of auditory, visual, and (nonrespiratory) somatosensory evoked potentials. As such, these early-latency components may form part of an arousal mechanism that protects against respiratory pathology during sleep. Long-latency RREP components, although still present during sleep, are reflected in patterns different from those seen in wakefulness and as such may play a different role during sleep. The exact mechanisms of this role, however, are yet to be determined.

Address for reprint requests: I. Colrain, Dept. of Psychology, The Univ. of Melbourne, Parkville, Victoria 3052, Australia (E-mail: colrain@psych.unimelb.edu.au).

Received 7 November 1997; accepted in final form 24 June 1998.

REFERENCES

1. **Addy, R. O., D. S. Dinner, H. Lüders, R. P. Lesser, H. H. Morris, and E. Wyllie.** The effects of sleep on medial nerve short latency somatosensory evoked potentials. *Electroencephalogr. Clin. Neurophysiol*. 74: 105–111, 1989.
2. **Campbell, K., I. Bell, and C. Bastien.** Evoked potential measures of information processing during natural sleep. In: *Sleep Arousal and Performance*, edited by R. Broughton and R. Ogilvie. Cambridge, MA: Birkhouser, 1992, p. 88–116.
3. **Campbell, K. B., and E. A. Bartoli.** Human auditory evoked potentials during natural sleep: the early components. *Electroencephalogr. Clin. Neurophysiol*. 65: 142–149, 1986.
4. **Colrain, I. M., J. Trinder, and G. Fraser.** Ventilation during sleep onset in young adult females. *Sleep* 13: 491–501, 1990.
5. **Colrain, I. M., J. Trinder, G. Fraser, and G. V. Wilson.** Ventilation during sleep onset. *J. Appl. Physiol*. 63: 2067–2074, 1987.
6. **Colrain, I. M., K. Webster, and G. Hirst.** Multi-channel EEG analysis of respiratory and auditory evoked potentials while awake and in NREM sleep (Abstract). *J. Sleep Res*. 5: 39, 1996.
7. **Davenport, P. W., I. M. Colrain, and P. M. Hill.** Scalp topography of the short-latency components of the respiratory-related evoked potential in children. *J. Appl. Physiol*. 80: 1785–1791, 1996.
8. **Davenport, P. W., W. A. Friedman, F. J. Thompson, and O. Franzen.** Respiratory-related cortical potentials evoked by inspiratory occlusion. *J. Appl. Physiol*. 60: 1843–1848, 1986.
9. **Davenport, P. W., G. A. Holt, and P. M. Hill.** The effect of increased inspiratory drive on the sensory activation of the cerebral cortex by inspiratory occlusion. In: *Respiratory Control: Central and Peripheral Mechanisms*, edited by D. F. Speck, M. S. Dekin, W. R. Revelette, and D. T. Frazier. Lexington: Univ. of Kentucky Press, 1992, p. 216–221.
10. **Davenport, P. W., R. Shannon, A. Mercak, R. L. Reep, and B. G. Lindsey.** Cerebral cortical evoked potentials elicited by cat intercostal muscle mechanoreceptors. *J. Appl. Physiol*. 74: 799–804, 1993.
11. **Davenport, P. W., F. J. Thompson, R. L. Reep, and A. N. Freed.** Projection of phrenic nerve afferents to the cat sensorimotor cortex. *Brain Res*. 328: 150–153, 1985.
12. **De Lugt, D. R., D. H. Loewy, and K. B. Campbell.** The effect of sleep onset on event related potentials with rapid rates of stimulus presentation. *Electroencephalogr. Clin. Neurophysiol*. 98: 484–492, 1996.
13. **Dempsey, J. A., K. G. Henke, and J. B. Skatrud.** Regulation of ventilation and respiratory function in NREM sleep. *Prog. Clin. Biol. Res*. 345: 145–154, 1990.
14. **Emerson, R. G., J. A. Sgro, T. A. Pedley, and W. A. Hauser.** State-dependent changes in the N20 component of the medial nerve somatosensory evoked potential. *Neurology* 38: 64–68, 1988.

15. **Gora, J., J. Trinder, A. Kay, I. M. Colrain, and J. Kleiman.** Load compensation as a function of state during sleep onset. *J. Appl. Physiol*. 84: 2123–2131, 1998.
16. **Harver, A., N. Squires, E. Bloch-Salisbury, and E. Katkin.** Event-related potentials to airway occlusion in young and old subjects. *Psychophysiology* 32: 121–129, 1995.
17. **Henke, K. G., M. S. Badr, J. B. Skatrud, and J. A. Dempsey.** Load compensation and respiratory muscle function during sleep. *J. Appl. Physiol*. 72: 1221–1234, 1992.
18. **Kay, A., J. Trinder, G. Bowes, and Y. Kim.** Changes in airway resistance during sleep onset. *J. Appl. Physiol*. 76: 1600–1607, 1994.
19. **Knafelc, M., and P. W. Davenport.** Relationship between inspiratory resistive loads and the P_1 peak amplitude of the respiratory related evoked potential. *J. Appl. Physiol*. 83: 918–926, 1997.
20. **Logie, S. L.** *Source Localisation of the Early Components of the Respiratory-Related Evoked Potential* (Masters thesis). Parkville, Australia: The University of Melbourne, 1997.
21. **Nielsen-Bohlman, L., R. T. Knight, D. L. Woods, and K. Woodward.** Differential auditory processing continues during sleep. *Electroencephalogr. Clin. Neurophysiol*. 79: 281–290, 1991.
22. **Noguchi, Y., T. Yamada, M. Yeh, M. Matsubara, Y. Kokubun, J. Kawada, G. Shiraishi, and S. Kajimotos.** Dissociated changes of frontal and parietal somatosensory evoked potentials in sleep. *Neurology* 45: 154–160, 1995.
23. **Ogilvie, R. D., I. A. Simons, R. H. Kuderian, T. Mac Donald, and J. Rustenberg.** Behavioural, event-related potentials, and EEG/FFT changes at sleep onset. *Psychophysiology* 28: 54–64, 1991.
24. **Orem, J.** The nature of the wakefulness stimulus for breathing. *Prog. Clin. Biol. Res*. 345: 23–30, 1990.
25. **Peterson, N. N., C. E. Schroeder, and J. C. Arezzo.** Neural generators of early cortical somatosensory evoked potentials in the awake monkey. *Electroencephalogr. Clin. Neurophysiol*. 96: 248–260, 1995.
26. **Rechtschaffen, A., and A. Kales** (Editors). *A Manual of Standardized Terminology, Techniques and Scoring Systems for Sleep Stages of Human Subjects*. Washington, DC: Govt. Printing Office, 1968.
27. **Revelette, W. R., and P. W. Davenport.** Effects of timing of inspiratory occlusion on cerebral evoked potentials in humans. *J. Appl. Physiol*. 68: 282–288, 1990.
28. **Strobel, R. J., and J. A. Daubenspeck.** Early and late respiratory-related cortical potentials evoked by pressure pulse stimuli in humans. *J. Appl. Physiol*. 74: 1484–1491, 1993.
29. **Trinder, J., F. Whitworth, A. Kay, and P. Wilkin.** Respiratory instability during sleep onset. *J. Appl. Physiol*. 73: 2462–2469, 1992.
30. **Wheatley, J. R., and D. P. White.** Influence of NREM sleep on respiratory-related cortical evoked potentials in normal humans. *J. Appl. Physiol*. 74: 1803–1810, 1993.